ARMY RESEARCH LABORATORY

Materials Characterization of High-Temperature Epoxy Resins: SC-79 and SC-15/SC-79 Blend

by Michael L. Wang, Ian M. McAninch, and John J. La Scala

ARL-TR-5484 March 2011

NOTICES

Disclaimers

The findings in this report are not to be construed as an official Department of the Army position unless so designated by other authorized documents.

Citation of manufacturer's or trade names does not constitute an official endorsement or approval of the use thereof.

Destroy this report when it is no longer needed. Do not return it to the originator.

Army Research Laboratory
Aberdeen Proving Ground, MD 21005-5069

ARL-TR-5484 **March 2011**

Materials Characterization of High-Temperature Epoxy Resins: SC-79 and SC-15/SC-79 Blend

Michael L. Wang and Ian M. McAninch
Oak Ridge Institute for Science and Education

John J. La Scala
Weapons and Materials Research Directorate, ARL

REPORT DOCUMENTATION PAGE	Form Approved OMB No. 0704-0188

1. REPORT DATE *(DD-MM-YYYY)*	2. REPORT TYPE	3. DATES COVERED (From - To)
March 2011	Final	April 2009–September 2010

4. TITLE AND SUBTITLE
Materials Characterization of High-Temperature Epoxy Resins: SC-79 and SC-15/SC-79 Blend

5a. CONTRACT NUMBER

5b. GRANT NUMBER

5c. PROGRAM ELEMENT NUMBER

6. AUTHOR(S)
Michael L. Wang,* Ian M. McAninch,* and John J. La Scala

5d. PROJECT NUMBER
H84

5e. TASK NUMBER

5f. WORK UNIT NUMBER

7. PERFORMING ORGANIZATION NAME(S) AND ADDRESS(ES)
U.S. Army Research Laboratory
RDRL-WMM-C
Aberdeen Proving Ground, MD 21005-5069

8. PERFORMING ORGANIZATION REPORT NUMBER
ARL-TR-5484

9. SPONSORING/MONITORING AGENCY NAME(S) AND ADDRESS(ES)

10. SPONSOR/MONITOR'S ACRONYM(S)

11. SPONSOR/MONITOR'S REPORT NUMBER(S)

12. DISTRIBUTION/AVAILABILITY STATEMENT
Approved for public release; distribution is unlimited.

13. SUPPLEMENTARY NOTES
*Oak Ridge Institute for Science and Education, 4692 Millennium Drive, Suite 101, Belcamp, MD 21017

14. ABSTRACT
The relatively low glass transition temperature (Tg) of the Army's SC-15 epoxy resin system necessitates study into suitable alternative resins capable of better low- and high-temperature performance. This work investigates two of those alternative resins, SC-79 and CCMFCS2, a blend of SC-15 and SC-79, both manufactured by Applied Poleramic Inc. (Benicia, CA). The viscosities and gel times of these resins are similar to SC-15's, thus substitution of the SC-15 with SC-79 or CCMFCS2 would cause no processing issues. Several different curing cycles were tested for each resin in an effort to find the best process for U.S. Army applications. Three slow cure cycles showed no meaningful advantages over faster, elevated temperature cures. Under all tested cure conditions, both SC-79 and CCMFCS2 are able to achieve higher Tg's and similar or greater flexural properties than SC-15; however, SC-15's fracture and impact properties were superior.

15. SUBJECT TERMS
epoxy, resin, composite

16. SECURITY CLASSIFICATION OF:			17. LIMITATION OF ABSTRACT	18. NUMBER OF PAGES	19a. NAME OF RESPONSIBLE PERSON
a. REPORT	b. ABSTRACT	c. THIS PAGE			Ian M. McAninch
Unclassified	Unclassified	Unclassified	UU	34	19b. TELEPHONE NUMBER (*Include area code*) 410-306-2134

Standard Form 298 (Rev. 8/98)
Prescribed by ANSI Std. Z39.18

Contents

List of Figures

List of Tables

Acknowledgments

This research was supported in part by an appointment to the Postgraduate Research Participation Program at the U.S. Army Research Laboratory (ARL) administered by the Oak Ridge Institute for Science and Education through an interagency agreement between the U.S. Department of Energy and ARL.

1. Introduction/Background

Composite materials are of high importance to the U.S. Army because they can be made lighter and stronger than their metallic counterparts. These materials are finding their way into everything from personal body armor and vehicle frames for ballistic protection to panels for structural support. Lighter loads mean more fuel economy, greater mobility, and less fatigue on the troops in the field. But it is also important that these materials be strong enough to satisfy their primary mission, be it a structural or ballistic resistance application.

SC-15 is a high-performance resin being considered for a number of Army composite applications. SC-15 is a toughened commercial vacuum-assisted resin transfer molding (VARTM) resin produced by Applied Poleramic Inc. (API) (Benicia, CA). It is a low-viscosity, two-phase toughened epoxy cured with a cycloaliphatic amine. This resin system was designed to work very well in VARTM processes and has good damage resistance in structural and ballistic applications. However, the relatively low glass transition temperature (Tg) of ~95 °C (*1*) has limited its use in many U.S. Army applications. Yet, other properties of this resin are excellent, including high resin and composite modulus, strength, toughness, and interlaminar shear strength (*2*). Therefore, the Army has been looking into using higher Tg resin systems that otherwise are similar to that of SC-15. Two candidate resin systems include SC-79 and CCMFCS2, both supplied by API.

SC-79 is a low-viscosity, two-phase toughened, cycloaliphatic amine–cured commercial VARTM resin system designed to be easy to handle and have a long processing window for large part assembly. According to the technical specification sheet, this resin has a Tg of ~145–165 °C for the low-temperature cure cycle and 170–194 °C for the high-temperature cure cycle (*3*).

CCMFCS2 is a blend of SC-15 and SC-79. As expected, this blend is a toughened low-viscosity epoxy resin, capable of VARTM composite manufacture. The technical specification sheet states a Tg of 130 °C (*4*).

While both SC-79 and CCMFCS2 are stated to have higher Tg's than SC-15, there are potential issues with the use of these resins. First, the technical data sheet for SC-79 list two potential cure schedules. To select the ideal cure schedule for U.S. Army applications, the effects of the cure schedule on morphology and thermal and mechanical properties must be determined. Second, the CCMFCS2 resin is recommended to be cured for 16–32 h at room temperature (RT) prior to a post-cure at an elevated temperature (*4*). This cure time is exceedingly long and can lead to processing problems including air leaks and high void fractions, as well as low production rates. Also, the RT cure schedule is unusual considering that the two resins it is composed of have recommended cures at 60 °C. However, modifying the cure schedule can have a deleterious

effect on the properties of resins, especially phase-separating toughened systems. Thus we evaluated the various cure schedules and characterized the mechanical properties of the resulting resins by characterizing the resins' rheological, calorimetric, dynamic mechanical, flexural, fracture, impact, and morphological properties and comparing the results to those of SC-15.

2. Experiment

2.1 Materials and Resin Formulation

According to SC-15's technical specification sheet (*5*), the resin is to be mixed thoroughly in a 100:30 resin-to-hardener (R:H) ratio by weight and then cured at 60 °C for 2 h before an additional post-cure of 4 h at 93.3 °C. For ease of processing and the purpose of this study, the post-cure cycle was changed to 100 °C for 3 h.

According to the specification sheet (*3*), SC-79 is mixed at a 100:40 R:H ratio by weight, cured at 60 °C for 4 h, and then post-cured at either 121 °C or 177 °C for 1 h (table 1), depending on the desired properties. The 121 °C cure was designed to meet Boeing Material Specification 8–79, 8168, 219, and to have better mechanical performance, especially "after hot-wet conditioning" with only slightly lower fracture toughness than the qualified pre-preg. In this study we investigated both cure cycles to evaluate their mechanical properties after each cycle.

Table 1. SC-79 cure cycles.

Cure Schedule	Cure	Post-Cure
Cycle 1	Ramp 10 °C/min to 60 °C, hold for 4 h	Ramp 10 °C/min to 121 °C, hold for 1 h
Cycle 2	Ramp 10 °C/min to 60 °C, hold for 4 h	Ramp 10 °C/min to 177 °C, hold for 1 h

The blend of SC-15/SC-79 VARTM resins, CCMFCS2, is recommended to be mixed in a 100:37.5 R:H ratio by weight (*4*). The suggested cure is 16–32 h at RT, with a post-cure consisting of a ramp of 1 °C/min to 121 °C. For the purpose of this study, the cure was standardized to a 24-h cure before a post-cure ramp of 1ºC/min to 121 ºC. Because the 24-h RT cure is not an ideal production cure schedule, an alternate cure cycle of 60 °C for 4 h was also tested. In addition to the recommended post-cure cycle, two additional post-cure cycles were tested; a 1 °C/min ramp to 145 °C followed by 2 h at 145 °C and a 1 °C/min to 177 °C followed by 1 h at 177 °C. Samples were made in all combinations of cure and post-cure cycles (table 2).

Table 2. CCMFCS2 cure cycles.

Cure Schedule	Cure	Post-Cure
Cycle 1	Hold for 24 h at RT	Ramp 1 °C/min to 121 °C, hold for 4 h
Cycle 2	Hold for 24 h at RT	Ramp 1 °C/min to 145 °C, hold for 2 h
Cycle 3	Hold for 24 h at RT	Ramp 1 °C/min to 177 °C, hold for 1 h
Cycle 4	Ramp 10 °C/min to 60 °C, hold for 4 h	Ramp 1 °C/min to 121 °C, hold for 4 h
Cycle 5	Ramp 10 °C/min to 60 °C, hold for 4 h	Ramp 1 °C/min to 145 °C, hold for 2 h
Cycle 6	Ramp 10 °C/min to 60 °C, hold for 4 h	Ramp 1 °C/min to 177 °C, hold for 1 h

2.2 Resin Characterization

2.2.1 Rheology

Viscosity and gel times of the curing resins were measured on a TA Instruments AR-2000 Rheometer at 25 °C and 60 °C with the temperature controlled by a Peltier plate. A parallel plate geometry with a 40-mm plate and a gap distance of 1000 μm was used for all the samples. Immediately prior to measurement, each resin was blended in the proper ratios and thoroughly mixed. Viscosity was then measured as a function of time at a shear rate of 1 s^{-1} and the shear stress was measured every 2 s. The viscosity was measured until the sample viscosity exceeded 5000 cP or until 300 min had past. A repeat run was performed for all the samples. The reported viscosity is an average of the first plateau region, generally the first 5 min of data or less if a noticeable viscosity change occurred.

2.2.2 Differential Scanning Calorimetry

A TA Instruments Q1000 differential scanning calorimeter (DSC) was used to measure the heat of reaction during the various cure cycles and determine the extent of cure. Approximately 10 mg of freshly mixed resin was sealed in aluminum hermetic DSC pans. Each heating ramp tested corresponds to an experimental cure cycle, as mentioned before, with additional steps to measure any residual cure. The general DSC procedure is as follows:

1. A heat ramp of 10 °C/min from 25 °C to the cure temperature followed by an isothermal hold at the cure temperature for its respective curing time.
2. A heat ramp of 1 °C/min from the cure temperature to its post-curing temperature, followed by an isothermal hold for the length of the post-cure cycle.
3. Heat at a rate of 10 °C/min to 200 °C and hold for 30 min to measure any residual cure before cooling down to RT again.
4. A final ramp of 10 °C/min to 200 °C to verify complete reaction.

We chose this method to examine the heat of cure during the cure cycle and determine whether there is further curing in the resin after being subjected to temperatures above its post-curing temperature. The extent of cure, α, can be determined using equation 1 (*6*):

$$\alpha = 1 - \frac{Q_{resid}}{Q_{tot}}, \quad (1)$$

where Q_{resid} is the residual heat generated during step 3, and Q_{tot} is the total heat of reaction.

Q_{tot} is difficult to measure because of a shifting baseline from the multiple steps; instead, Q_{tot} was determined by taking ~10 mg of freshly mixed, uncured sample and measuring the total heat during a 5 °C/min ramp from RT to 250 °C. Complete reaction was assumed and an average of four runs was used.

2.2.3 Dynamic Mechanical Analysis (DMA)

A TA Instruments Q800 dynamic mechanical analyzer with a 35-mm dual cantilever clamp was used to characterize the resins' storage modulus (E'), loss modulus (E'') peak, and tan δ maximum temperature. DMA applies an oscillatory strain to the sample and measures its material response to that force. Samples had rectangular dimensions of ~60 × 12 × 3 mm. Temperature ramps from 25 °C to 200 °C at a rate of 2 °C/min with an oscillation frequency of 1 Hz and a displacement of 7.5 μm were used for the SC-79. Similarly the CCMFCS2 samples were measured at the same frequency and displacement from 25 °C to at least 180 °C while SC-15 was tested up to 160 °C. The upper temperature limits were chosen to characterize the materials up to and through their Tg's but not necessarily well beyond. The resins were compared on the basis of storage modulus, loss modulus peak(s), and the temperature where the maximum occurred in tan δ. The Tg of the material was taken as the temperature where the peak of the loss modulus, E", curve occurred. In the case that multiple peaks exist, as in a phase-separated system, the higher temperature, or second peak, was taken as the Tg.

In addition to the dry specimens, wet DMA samples were tested to ascertain the susceptibility of these resins to water absorption and characterize how water absorption affects material properties. These samples were submersed in 90 °C water for 24 h, after which the samples were removed from the water, blotted dry, and then immediately tested using the appropriate DMA procedure as described previously.

2.2.4 Flexural Testing

Three-point bend resin characterization was performed using an Instron 5500R equipped with a 5-kN load cell. Both the supports and loading nose had cylindrical surfaces. Testing was done according to ASTM standard D 790-03 (*7*). Samples were cut from cast sheets for flatwise testing, with the sample span being 16× (tolerance ±1) the depth of the beam. Specimen depth was taken to be the depth at the center of the beam. Nominal sample dimensions were ~75 × 12 × 4 mm. The rate of crosshead motion was calculated by equation 2.

$$R = \frac{ZL^2}{6d} \quad , \tag{2}$$

where:

R = rate of crosshead motion (mm/min).

L = support span (mm).

d = depth of beam (mm).

Z = rate of straining of the outer fiber (mm/mm/min).

For our calculations, procedure B (*7*) with Z = 0.1 was used. The nominal crosshead speed was 23.4 mm/min.

2.2.5 Fracture Toughness

Fracture testing was performed according to ASTM standard D 5045-93 (*8*) using the single-edge-notch bending geometry. The resin was cured in a 76- × 89- × 12.7-mm open mold, and a notch equal to half the thickness was machined through the entire block with one cut. Individual test specimens with nominal dimensions of 89 × 6.4 × 12.7 mm were cut from the block. A fresh crack was initiated in the samples immediately before testing by drawing a sharp razor blade through the machined notch. Each razor blade was used no more than three times. Samples were tested on an Instron testing machine with a crosshead speed of 1.27 mm/min and a span of 50.8 mm. An unnotched sample was tested according to the standard to account for system compliance, loading pin penetration, and sample compression. The fracture surfaces were examined for signs of plastic deformation, and any sample with noticeable deformation was not included in the results.

2.2.6 Izod Impact Testing

Notched Izod impact testing was performed according to ASTM standard D 256-05 (*9*). Samples were made using a mold that contains the notch made to the specified dimensions; this prevents microcracking or other damage from occurring if one were to machine the notch. The samples were ~63.5 × 12.7 × 12.7 mm, excluding the notch. Unnotched Izod impact testing was also performed according to ASTM D 4812-99 (*10*). Rectangular samples with dimensions of ~63.5 × 12.7 × 3.17 mm were cut from cast sheets. Both types of samples were tested on an Instron POE 2000 using Impulse data acquisition software.

2.2.7 SEM Characterization

A JEOL JSM 6460LV scanning electron microscope (SEM) was used to characterize the morphology of the resins to compare similarities and differences among curing cycles. These morphologies were compared to SC-15. DMA samples were fractured to expose internal surfaces. The surfaces were then sputtered with a thin layer of gold using a Denton Desk IV sputter coater (Moorestown, NJ).

3. Results

Note that all samples, regardless of the cure schedule, were white in color and opaque. Opacity is a visible sign of phase separation, where the secondary phase forms domains large enough to scatter light, whereas nontoughened resins tend to be transparent (*11*).

3.1 Rheology Analysis

The time to reach 5000 cP was measured and considered to be the gel time, as after that point VARTM processing is no longer feasible. Materials with gel times ranging from 45 min to 2 h are ideal for Army applications.

Previous U.S. Army Research Laboratory (ARL) work has verified that SC-15 processes easily; the viscosities of SC-15, SC-79, and CCMFCS2 are shown in table 3. All three have similar viscosities at 25 °C as well at as 60 °C. The viscosities reported here are slightly higher than those reported on the data sheets (*3–5*), but the differences can be attributed to aging that occurred after receipt of the resins.

Table 3. Initial viscosities and time to reach 5000 cP at processing temperatures.

Resins	Initial Viscosity at 25 °C (cP)	Time to 5000 cP at 25 °C (min)	Initial Viscosity at 60 °C (cP)	Time to 5000 cP at 60 °C (min)
SC-15 (*1*)	508 ± 60	301	47 ± 8	73
SC-79	437 ± 42	300+	44 ± 8	75 ± 7
CCMFCS2	449 ± 47	300+	47 ± 8	66 ± 5

This work finds that all three resin systems have suitable working viscosities in which VARTM processing is practical for Army applications; however, the very slow viscosity increases at RT can give rise to problems, such as vacuum leaks during the long RT cure. The cures at 60 °C offer a much more useful cure schedule, providing gel times well within the acceptable range. Furthermore, all resins had similar gel times at 60 °C, and thus substitution of the SC-15 with SC-79 or CCMFCS2 would cause no processing issues.

3.2 Differential Scanning Calorimetry Analysis

The total heats of reaction for SC-79 and CCMFCS2 were measured to be 434 ± 17 J/g and 416 ± 8 J/g, respectively. Using these data and the measured ΔH_{resid}, we calculated the extents of cure for each resin cycle and summarized the results in table 4.

Table 4. Extent of cure by DSC.

Cure Schedule	ΔH_{resid} (J/g)	Extent of Cure (Cure + PC) (%)
SC-79		
Cycle 1	40	90.86 ± 0.35
Cycle 2	21	95.11 ± 0.19
CCMFCS2		
Cycle 1	13	96.90 ± 0.06
Cycle 2	4	99.03 ± 0.02
Cycle 3	6	98.67 ± 0.03
Cycle 4	10	97.71 ± 0.04
Cycle 5	3	99.32 ± 0.01
Cycle 6	2	99.50 ± 0.01

For cycle 1 of SC-79, the extent of cure is somewhat low at 91%; this is not surprising given that the post-cure temperature of 121 °C is well below the maximum Tg of 170 °C reached with the 177 °C post-cure (*3*). For SC-79 cycle 2, the 95% extent of cure is more surprising, given that the post-cure exceeds the ultimate Tg. Since the resin is toughened, diffusion limitations could have trapped the unreacted monomer in its nonpreferred phase, limiting the reaction potential.

For CCMFCS2 cured at RT (cycles 1–3), raising the post-cure from 121 °C to 145 °C increased the extent of cure, while a further increase in post-cure temperature to 177 °C had no significant effect. The same trend was seen when the cure temperature was raised to 60 °C (cycles 4–6). Thus it can be concluded that 145 °C and higher post-cure temperatures allow for maximum mobility of the polymer reactive groups, while 121 °C post-cure is not completely above the vitrification temperature of the resin. The extent of cure was slightly higher when cured at 60 °C, again because of higher mobility of the reactive groups during cure.

3.3 DMA Analysis

The SC-15 material properties, as reported on the material specification sheet provided by API, lists a Tg of 104 °C and Tg (wet) of 81 °C (*5*). However, previous ARL work (*1*) finds that the Tg is 95 ± 1.5 °C with a Tg (wet) of 80 °C and a corresponding storage modulus (E') of 2.5 ± 0.1 GPa at 30 °C. Our experiments measured a Tg of 95.0 ± 0.7 °C, when the Tg is taken as the peak of the E'' curve and supports ARL's previous work. The maximum in the tan δ was found to be 108.3 ± 3.0 °C, which is very similar to the Tg reported by API. The E' we obtained was 2.2 ± 0.3 GPa, which is not significantly different from the previous study.

For the two SC-79 cure cycles, the materials specification sheet from API claims a Tg of 145–165 °C for the 121 °C cycle and 170–194 °C for the 177 °C cycle (*3*). It also reports Tg (wet) of 110 °C for the 121 °C cycle and 135–160 °C for the 177 °C cycle. Our results for the 121 °C cycle were 115.1 ± 1.5 °C and 2.6 ± 0.2 GPa for the Tg and 30 °C modulus, respectively. A second DMA run of the same samples raised the Tg to 141.7 ± 0.9 °C and the E' to 2.8 ± 0.3 GPa. This jump in Tg is the result of additional curing of the sample during the first run.

This agrees with the DSC results, showing incomplete reaction for the 121 °C cure. For the 177 ºC cycle, the Tg was 152.2 ± 2.5 ºC and the storage modulus 2.6 ± 0.1 GPa. A second run raised these values to 155.4 ± 5.8 ºC and 2.8 ± 0.1 GPa for the Tg and E', respectively. Here, the changes between the first and second DMA runs were minor, reflecting the more complete cure. As for the SC-15, the Tg's specified by API more closely match the temperature of the tan δ maximum.

In the DMA results for both cure cycles for SC-79, all E'' curves had a second peak, which indicates phase separation of the system, as shown in figure 1. The intensity of the peak varied, appearing as only a shoulder in the 121 °C cured samples and as a distinct peak in the 177 °C cured samples. The location of the peaks was similar: 69 ± 1 °C for the 121 °C cured samples vs. 74 ± 3 °C for the 177 °C cured samples. This secondary peak corresponds to a toughener-rich phase while the main higher-temperature peak corresponds to an epoxy-rich phase. Unfortunately, the data sheet does not give details on the nature of the toughener.

The higher-temperature post-cure allows the resin to more completely phase separate, yet it also significantly increases the higher-temperature loss modulus peak by 25 °C. Despite the higher Tg of the SC-79 resin post-cured at 177 °C up to ~90 °C, the resin post-cured at 121 °C has a similar modulus. For the wet cycle 1 samples, when comparing the dry DMA data to the wet DMA data (figure 2), the storage modulus is depressed and there are changes in the loss modulus curve. For the wet sample, the lower-temperature loss peak is much more intense than before and it occurs 20 °C lower, while the higher-temperature loss modulus peak has increased 10 °C. Two mechanisms could explain this behavior. First, the toughening phase could have a higher affinity for water than the epoxy phase; however, another study using carboxyl-terminated butadiene-acrylonitrile (CTBN)-toughened epoxy showed lower water absorption for toughened systems (*12*). Again, the lack of knowledge of the toughening phase limits insight. Second, the 24 h at 90 °C in water could give unreacted toughening monomers additional time to phase separate from the epoxy phase, or unreacted monomers could leach out from the polymer. Similar behavior was seen in a nontoughened epoxy: after 32 h in 80 °C the Tg increased ~5 °C, and after longer immersion times, the Tg increased ~15 °C (*13*). The wet cycle 2 samples had a depression of ~10 °C for both loss modulus peaks, and the modulus was lower for all temperatures relative to cycle 1. Wet and dry DMA data are summarized in table 5.

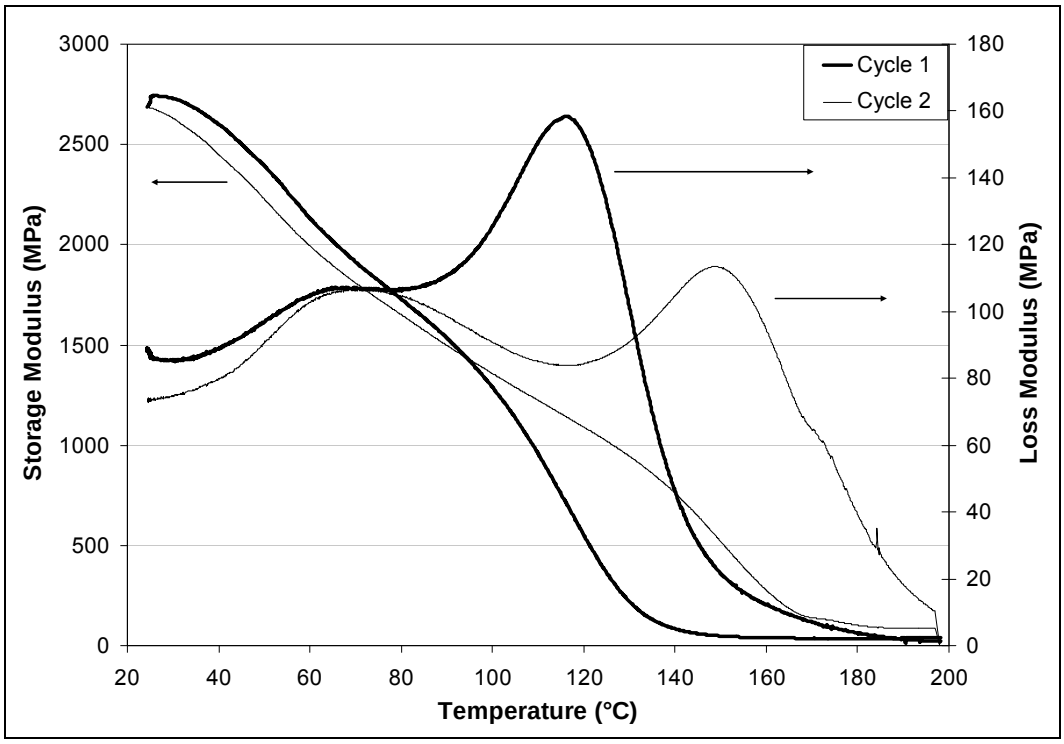

Figure 1. Storage and loss moduli of SC-79 post-cured at 121 °C (heavy line) and 177 °C (light line).

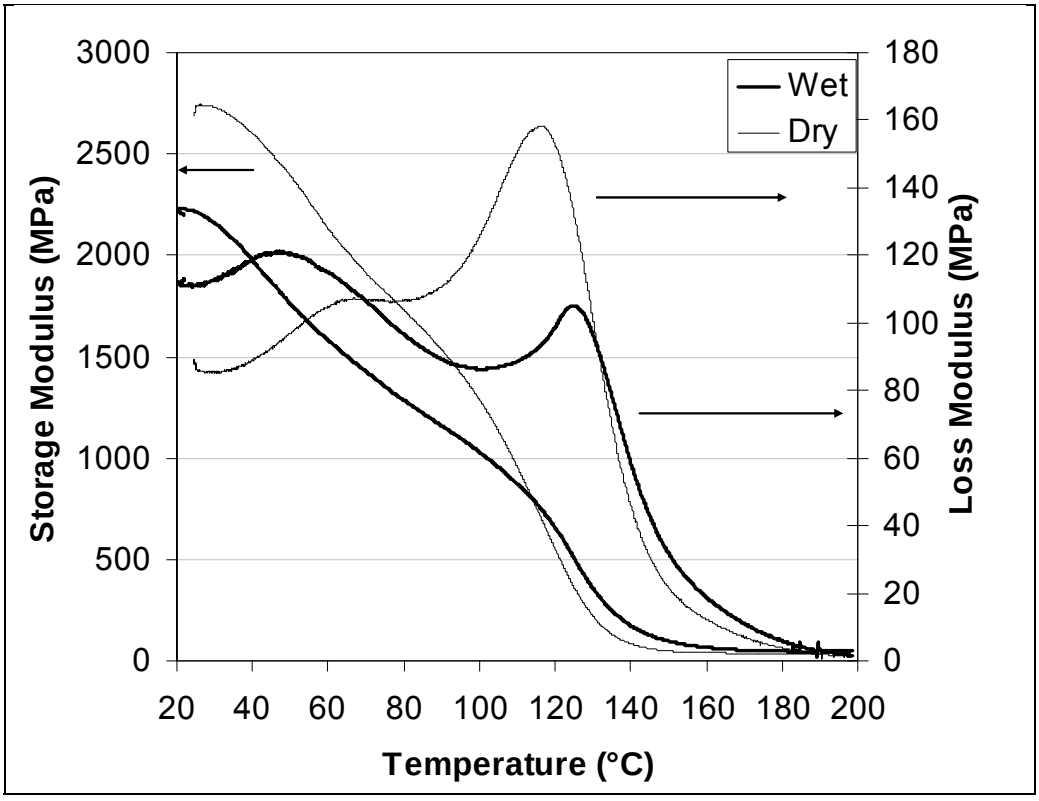

Figure 2. SC-79 cycle 1 after water immersion (heavy line) compared to SC-79 cycle 1 dry (light line).

Table 5. DMA results summary.

Cure Schedule	Tg	Loss Modulus Peaks (LM1/LM2) (°C)	Max tan δ (°C)	Wet Tg (LM1/LM2) (°C)	E' at 30 °C (MPa)
SC-15 (*1*)					
Single cycle	95.4 ± 1.5	– /95.4 ± 1.5	110.7 ± 1.0	– / 80	2.5 ± 0.1
SC-79					
Cycle 1	115.1 ± 2.0	67.8 ± 1/ 115.1 ± 2	138.6 ± 1.8	49.3 ± 2.8/ 125.3 ± 0.4	2.6 ± 0.2
Cycle 2	152.2 ± 3.0	74.2 ± 3/ 152.2 ± 3	175.2 ± 4.2	57.0/143.4	2.6 ± 0.1
CCMFCS2					
Cycle 1	119.3 ± 5.4	– /119.3 ± 5.4	137.8 ± 3.0	45.5 ± 4.3/ 107.0 ± 0.7	2.5 ± 0.1
Cycle 2	122.3 ± 1.0	– /122.3 ± 1.0	140.6 ± 0.8	56.4 ± 1.4/ 112.9 ± 0.8	2.3 ± 0.1
Cycle 3	130.0 ± 0.8	72.1 ± 2.7/ 130.0 ± 0.8	145.7 ± 0.5	58.3/120.3	2.2 ± 0.2
Cycle 4	121.4 ± 6.3	68.4 ± 3/ 121.4 ± 6.3	140.9 ± 3.0	52.8 ± 0.5/ 115.4 ± 1.1	2.1 ± 0.2
Cycle 5	128.2 ± 1.6	73.7 ± 5.8/ 128.2 ± 1.6	145.3 ± 0.5	54.7 ± 1.7/ 114.4 ± 5.8	2.5 ± 0.1
Cycle 6	131.9 ± 3.3	74.7 ± 3.2/ 131.9 ± 3.3	148.0 ± 2.0	57.9 ± 0.4/ 122.0 ± 3.6	2.2 ± 0.1

The datasheet of the blend, CCMFCS2, reported a Tg of 130 °C and a wet Tg of 118 °C for cycle 1. This cure cycle resulted in a Tg of 119.3 ± 5.4 °C, a storage modulus of 2.5 ± 0.1 GPa at 30 °C, and a maximum in tan δ at 137.8 ± 3.0 °C, again suggesting that the reported Tg is the peak of the tan δ curve rather than the loss modulus. Cycles 2 and 3 yielded Tg's of 122.3 ± 1.0 °C and 130.0 ± 0.8 °C with storage moduli of 2.3 ± 0.1 GPa and 2.2 ± 0.2 GPa, respectively. For the cycles cured using an accelerated time and elevated temperature schedule, cycle 4 resulted in a Tg of 121.4 ± 6.3 °C and a E' of 2.1 ± 0.2 GPa, while cycle 5 had a Tg of 128.2 ± 1.6 °C and E' of 2.5 ± 0.1 GPa, and cycle 6 had a Tg of 131.9 ± 3.3 and E' of 2.2 ± 0.1 GPa.

In most of the samples, there is evidence of a second peak similar to SC-79's phase separation (figure 3, light line). This secondary peak occurs around the same temperatures as the secondary peak in SC-79, 65–75 °C. In cycles 1 and 2, the secondary peak is only visible as a small shoulder on the main peak (figure 3, heavy line). SC-15 does not show a secondary loss peak in this temperature range, as illustrated in figure 4, so it is possible that the secondary loss peak in the CCMFCS2 is caused by the SC-79 toughener rather than SC-15's. Yet, SC-15's lower Tg would more likely result in a single, broader glass transition, whereas the larger difference between the loss modulus peaks of SC-79 and CCMFCS2 would likely be more visible as distinct transitions.

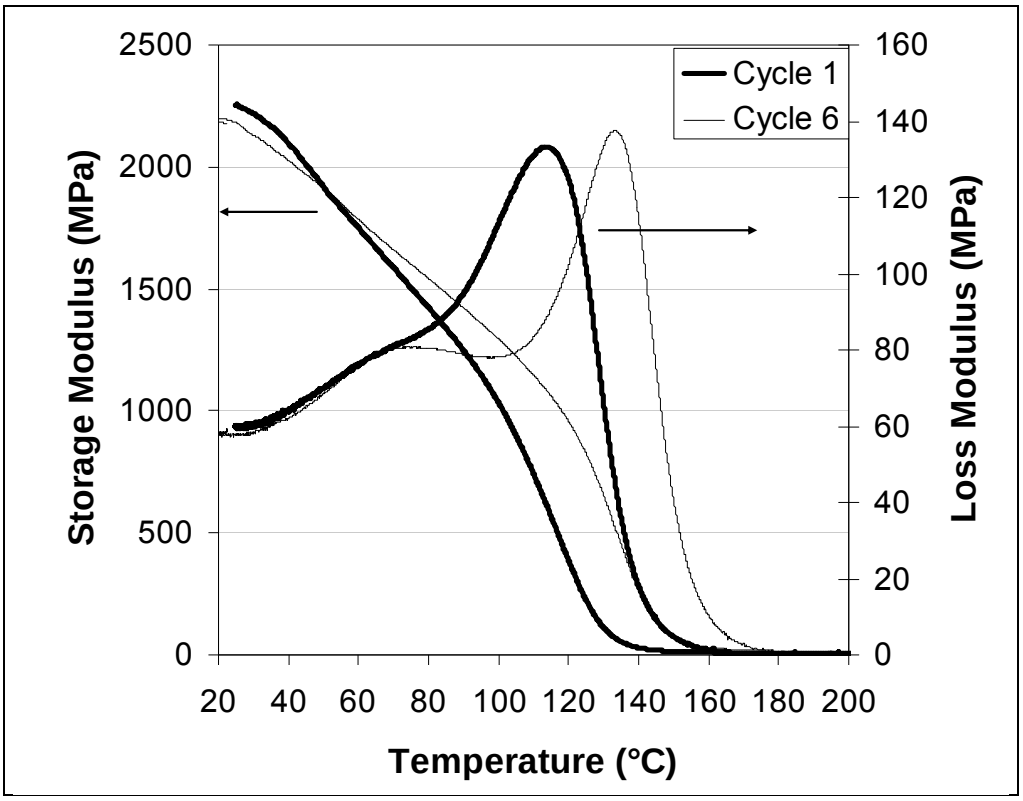

Figure 3. Storage and loss moduli of CCMFCS2: cycle 1 (heavy line) and cycle 6 (light line).

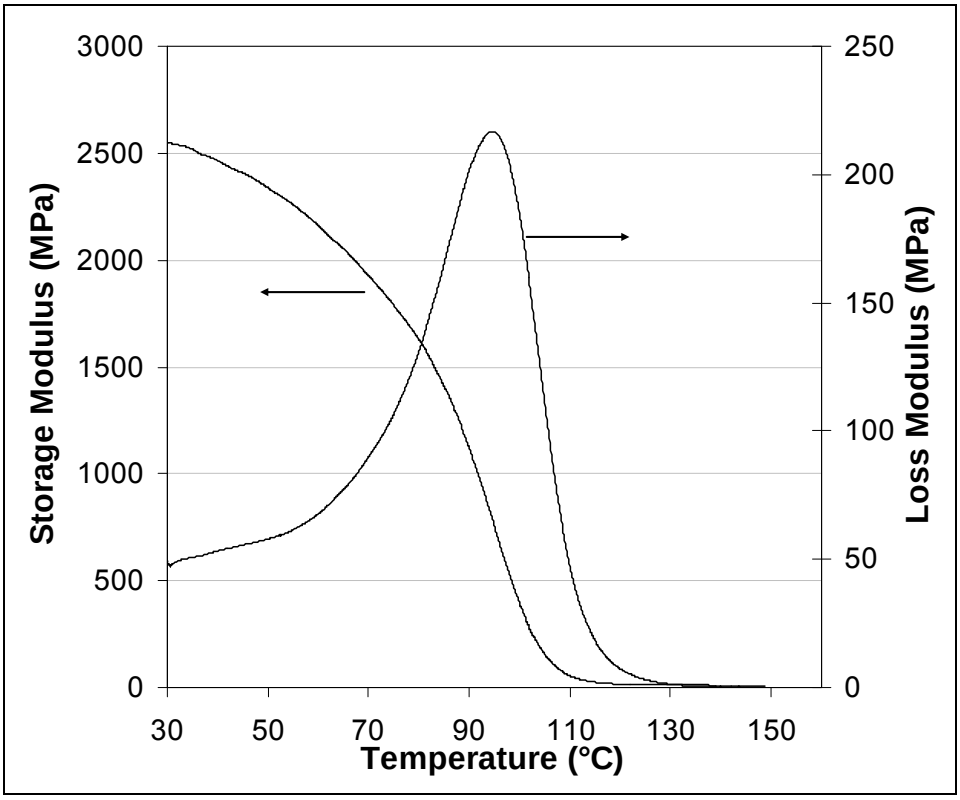

Figure 4. Storage and loss moduli curves for SC-15.

The DMA results show that Tg increases as the post-cure temperature increases. For cycles 1–3, the room-temperature-cured samples, there is a small increase in Tg comparing the 121 °C to the 145 °C post-cured samples; a larger increase occurs between post-cures of 145 and 177 °C. For cycles 4–6, the 60 °C cured samples, the largest change occurs between 121 and 145 °C post-cured samples, with 177 °C post-cured samples having a similar Tg as the 145 °C post-cured samples. These results agree with the DSC results. From table 4, cycles 1 and 4 had the lowest extents of cure, which corresponds to the lowest Tg's. The other four cycles have very similar extents of cures, but for small residual heats, the Tg changes can be a more accurate indicator of additional cure (*14*). Overall, the Tg trends agree with the extents of cure from DSC. Table 5 provides a summary of DMA results for SC-15, SC-79, and CCMFCS2.

All cycles show similar behavior after immersion in 90 °C water. The Tg was depressed by 6–14 °C with no trend between the cycles. The secondary loss peak also shifted to lower temperatures by 15–20 °C for all cycles. Wet Tg data are also summarized in table 5.

3.4 Flexural Results Analysis

The flexural strengths of the resins at various cure conditions are shown in table 6. SC-15 has a flexural modulus of 2.8 ± 0.1 GPa, a strength of 110 ± 2 MPa, and a strain at failure of 6.4 ± 0.3% (*1*). For SC-79 at 121 °C, we measured a flexural modulus of 2.6 ± 0.1 GPa, a strength of 106 ± 5 MPa, and a strain at failure of 5.8 ± 0.5%. With the 177 ºC cycle, we measured a modulus of 3.4 ± 0.1 GPa, a strength of 126 ± 2 MPa, and a strain at failure of 4.9% ± 0.5%. Of these flexural results, it appears as though cycle 2 (table 6) has superior performance, with higher strength (+20 MPa) and modulus (+800 MPa), with only a 1% reduction in strain at failure.

Table 6. Flexural properties of SC-79 and CCMFCS2.

Cure Schedule	Flexural Strength (MPa)	Flexural Modulus (GPa)	Strain at Failure (%)
SC-15 (*1*)			
Single cycle	110 ± 2	2.8 ± 0.1	6.4 ± 0.3
SC-79			
Cycle 1	106.2 ± 4.7	2.6 ± 0.1	5.8 ± 0.8
Cycle 2	126.2 ± 2.2	3.4 ± 0.1	4.9 ± 0.5
CCMFCS2			
Cycle 1	105.8 ± 2.6	2.4 ± 0.1	7.4 ± 0.8
Cycle 2	121.9 ± 7.4	3.0 ± 0.0	6.8 ± 1.8
Cycle 3	119.5 ± 7.8	2.9 ± 0.2	6.1 ± 0.9
Cycle 4	109.2 ± 6.6	2.6 ± 0.1	5.9 ± 0.9
Cycle 5	110.9 ± 5.0	2.6 ± 0.1	6.4 ± 0.8
Cycle 6	120.6 ± 1.7	2.7 ± 0.1	6.6 ± 0.4

CCMFCS2 cycle 1 resulted in a flexural modulus of 2.4 ± 0.1 GPa, a strength of 106 ± 3 MPa, and a strain at failure of 7.3 ± 0.7%, while cycle 2 resulted in a flexural modulus of 3.0 ± 0.0 GPa, a strength of 122 ± 7 MPa, and a strain at failure of 6.8 ± 1.8%. Cycle 3 resulted in a flexural modulus of 2.9 ± 0.2 GPa, a strength of 119 ± 8 MPa, and a strain at failure of 6.1 ± 0.9%. These results show that cycle 1, in addition to having the lowest Tg, also has the lowest flexural modulus and strength due to its lowest extent of cure. Cycle 2 is preferred to cycle 3, as both have essentially the same properties consistent with the similar extent of cure and thermomechanical properties, but cycle 2 uses a lower post-cure temperature. Cycles 4 and 5 both had flexural moduli of 2.6 ± 0.1 GPa, while cycle 6 had a flexural modulus of 2.7 ± 0.1 GPa. Their strengths were 109.2 ± 6.6, 110.9 ± 5.0, and 120.6 ± 1.7 MPa, respectively. Their strains at failure were 5.9 ± 0.9%, 6.4 ± 0.8%, and 6.6 ± 0.4%, respectively. In addition to having the highest Tg for the CCMFCS2 cycles, cycle 6 also has the highest flexural modulus and strength. Table 6 gives a summary of the flexural results for SC-15, SC-79, and CCMFCS2.

Comparing the data in tables 5 and 6, we see that SC-79 cycle 2 has the highest overall strength, modulus, and Tg, but it also has the lowest strain at failure by 1%–2%. CCMFCS2 cycle 6 is the second best with similar strength and better strain at failure, but with a lower modulus and a substantially lower Tg (20 °C lower than SC-79 cycle 2).

3.5 SEM Characterization

The extent and size of phase-separated domains were characterized using SEM. Figure 5 shows the phase separation in SC-15 at 5000 and 10,000× magnification. The toughening phase appears to be around 0.5–1 μm in size. Figure 6 shows the phase separation of SC-79 for both cycles. Again, the second phase is ~1 μm in size, but the concentration appears to be lower than in the SC-15. The morphology is not noticeably different between the 121 °C and the 177 °C post-cure.

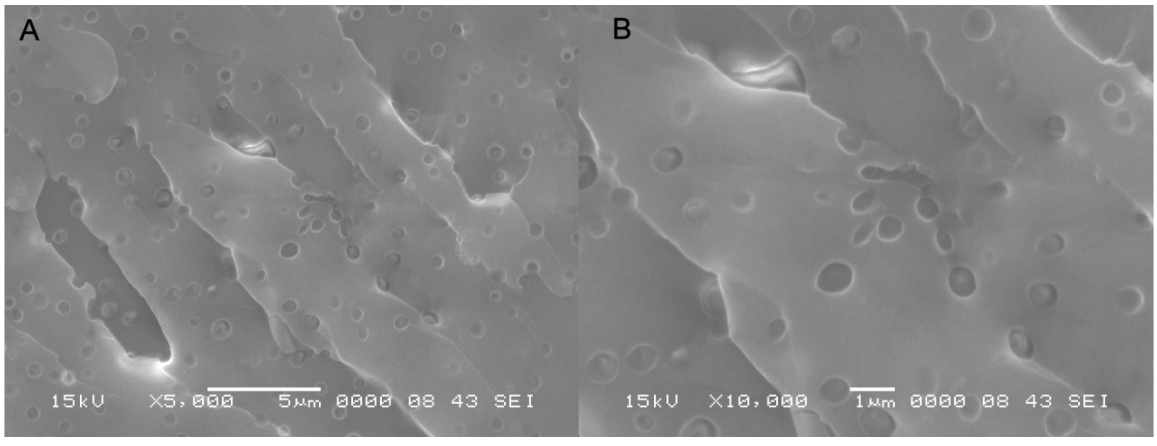

Figure 5. SEM image of SC-15 with the second toughened phase present at (A) 5000× and (B) 10,000× magnification.

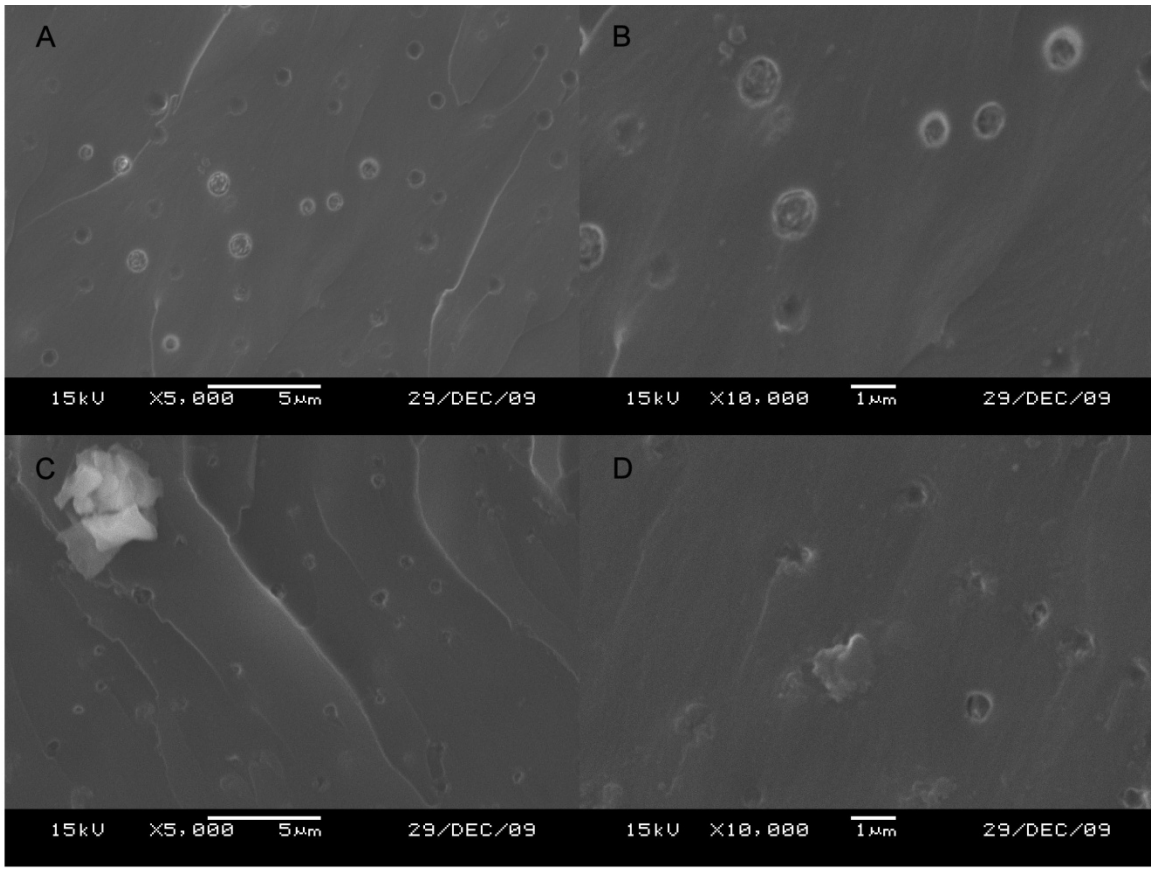

Figure 6. SEM images of SC-79 cycle 1 (A and B) and cycle 2 (C and D) at 5000× and 10,000× magnification.

Figure 7 shows the morphology of the CCMFCS2 resin cycles 1–3, those with a 24-h cure time. The second phase appears similar in size in all cycles, being ~0.5 µm in diameter with a concentration more similar to SC-15 rather than SC-79.

The morphology of the higher-temperature cured samples, cycles 4–6, is shown in figure 8. Again, the post-cure temperature causes little difference between the samples, with particle size ~1 µm, presumably because the morphology is locked in during the cure rather than the post-cure step. The concentration of particles is also more similar to SC-15 than SC-79.

Comparing figures 7 and 8, it appears that cycles 1–3 have more and smaller particles while cycles 4–6 have fewer and larger particles. While smaller particles have been shown to toughen epoxies better than larger particles (*15*), it is not clear that the small size difference is large enough to affect the fracture properties significantly (*15*, *16*).

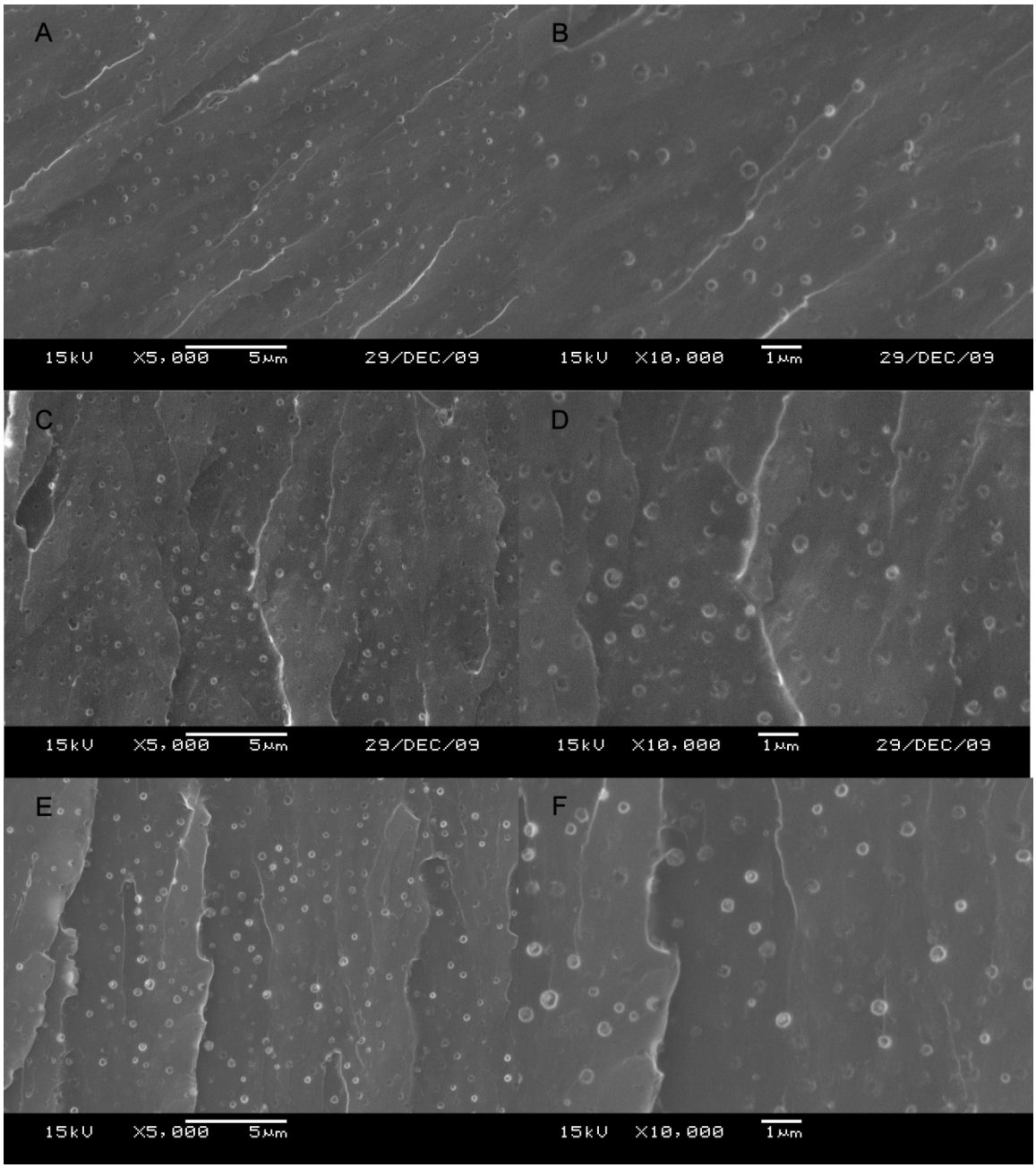

Figure 7. SEM of CCMFCS2 cycle 1 (A and B), cycle 2 (C and D), and cycle 3 (E and F) at 5000× and 10,000× magnification.

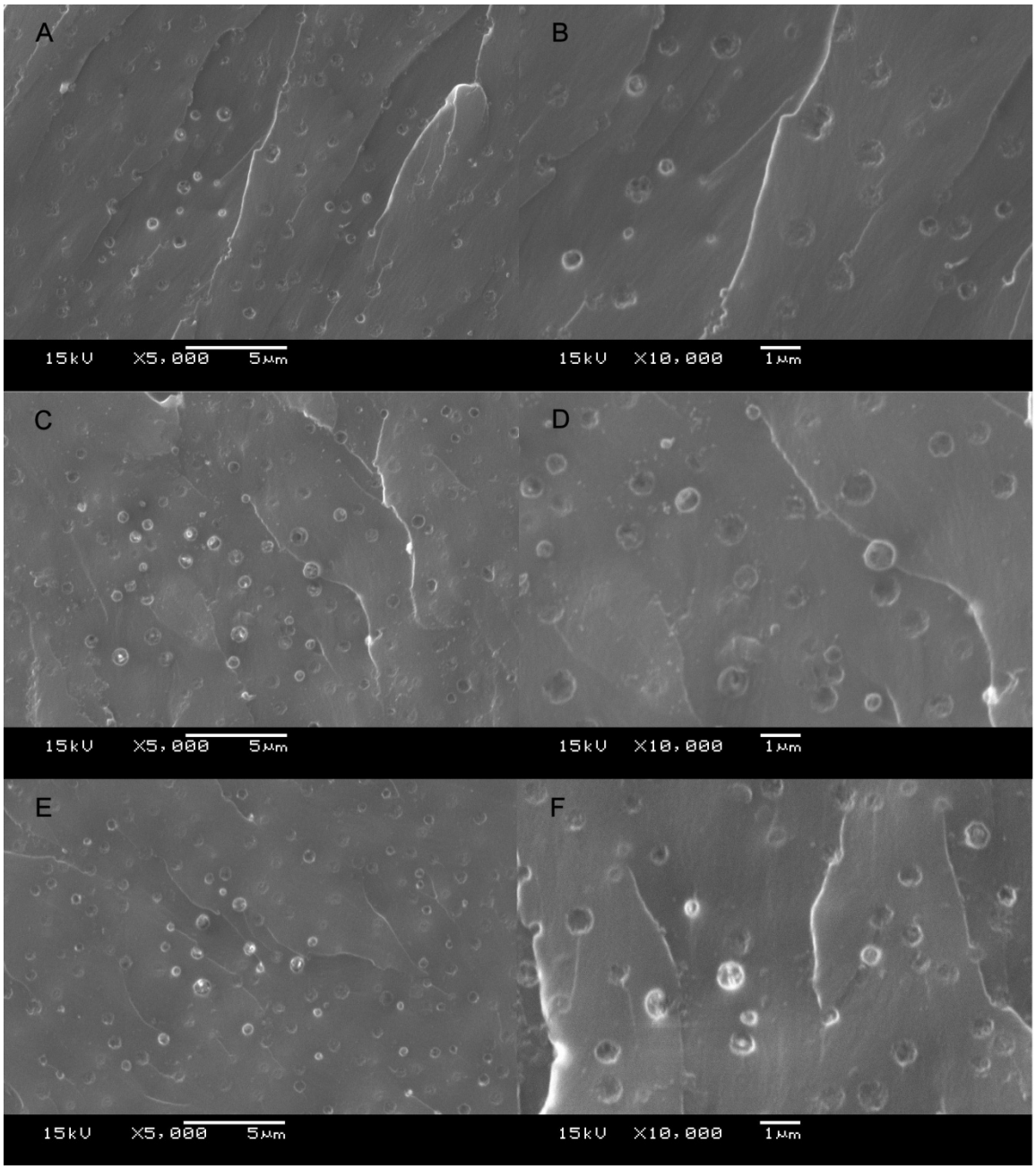

Figure 8. SEM images of CCMFCS2 cycle 4 (A and B), cycle 5 (C and D), and cycle 6 (E and F) at 5000× and 10,000× magnification.

3.6 Fracture Toughness Analysis

As the cure cycle can affect the morphology, so can the morphology influence toughness, especially in phase-separating systems. The extent of phase separation and size of the phase-separated domains can significantly affect the fracture toughness.

According to previous ARL work, SC-15 has a K_{1c} value of 2.08 ± 0.09 MPa·$m^{1/2}$ and a G_{1c} value of 1460 ± 120 J/m^2.

SC-79 cycle 1 has a K_{1c} value of 1.61 ± 0.25 MPa·$m^{1/2}$ and a G_{1c} of 1086 ± 267 J/m^2. Cycle 2, the higher-temperature post-cured cycle, had a much lower fracture toughness of K_{1c} 0.79 ± 0.19 MPa·$m^{1/2}$ and a G_{1c} value of 329 ± 122 J/m^2. A trend of increasing extent of cure and increasing post-cure temperature with decreasing overall fracture toughness is seen in this case. The unreacted monomer in SC-79 cycle 1 can plasticize the resin and improve fracture properties (*17*). With the higher post-cure of cycle 2, the extent of cure is increased, decreasing the amount of plasticizing monomers.

The CCMFCS2 room-temperature-cured resins, cycles 1–3, resulted in K_{1c} values of 1.28 ± 0.25 MPa·$m^{1/2}$, 1.12 ± 0.16 MPa·$m^{1/2}$, and 1.24 ± 0.14 MPa·$m^{1/2}$, respectively. Their G_{1c} values were 671 ± 225 J/m^2, 596 ± 163 J/m^2, and 742 ± 193 J/m^2, respectively. The elevated temperature-cured cycles, 4–6, resulted in K_{1c} values of 1.55 ± 0.13 MPa·$m^{1/2}$, 1.44 ± 0.22 MPa·$m^{1/2}$, and 1.24 ± 0.11 MPa·$m^{1/2}$, respectively. Their G_{1c} values were 855 ± 147 J/m^2, 977 ± 219 J/m^2, and 724 ± 123 J/m^2, respectively. Cycle 2 breaks from the trend of increasing post-cure temperature, leading to decreased fracture properties, but overall the samples post-cured at the lowest temperature have the highest fracture properties. The accelerated cured cycles (4–6) have, in general, higher fracture toughness values than the RT-cured cycles (1–3) even though they have higher extents of cure. A summary of all fracture values can be seen in table 7.

Table 7. Fracture property summary.

Cure Schedule	K_{1c} (MPa·$m^{1/2}$)	G_{1c} (J/m^2)	G_{1c} (J/m^2) from K_{1c}
SC-15 (*1*)			
Single cycle	2.08 ± 0.09	1460 ± 120	1533 ± 137
SC-79			
Cycle 1	1.61 ± 0.25	1086 ± 267	901 ± 288
Cycle 2	0.79 ± 0.19	329 ± 122	226 ± 116
CCMFCS2			
Cycle 1	1.28 ± 0.25	671 ± 225	652 ± 273
Cycle 2	1.12 ± 0.16	596 ± 163	480 ± 145
Cycle 3	1.24 ± 0.14	742 ± 193	610 ± 137
Cycle 4	1.55 ± 0.13	855 ± 147	1006 ± 175
Cycle 5	1.44 ± 0.22	977 ± 219	753 ± 224
Cycle 6	1.24 ± 0.11	724 ± 123	625 ± 104

Overall, SC-15 has the highest toughness, SC-79 cycle 1 has the second highest toughness, and SC-79 cycle 2 has the lowest toughness. SC-15's high toughness can partially be explained by its lower Tg. With similar toughening agents, the resin with the lowest cross-link density, and hence the lowest Tg, has been shown to have the highest fracture toughness (*18*). Conversely, SC-79 cured at 177 °C has the highest Tg and, assuming a similar concentration of toughening agent, would have the lowest fracture toughness. The high toughness from SC-79 cycle 1 most likely comes from the ~10% unreacted monomer coupled with the rubber toughening; an incomplete reaction can plasticize resins, leading to increased toughness (*17*). The other samples only had 0%–5% unreacted monomers.

3.7 Izod Impact Testing

Figure 9 shows the notched Izod impact testing data for all cycles of the CCMFCS2, along with SC-15 and both cycles for SC-79. Surprisingly, the impact data does not correlate with the fracture toughness measurements. Where SC-79 cycle 1 had the highest K_{1c} values, it has the second lowest for the impact test. For the CCMFCS2 samples, the impact resistance does not vary with the post-cure temperature; all values are very similar considering the error.

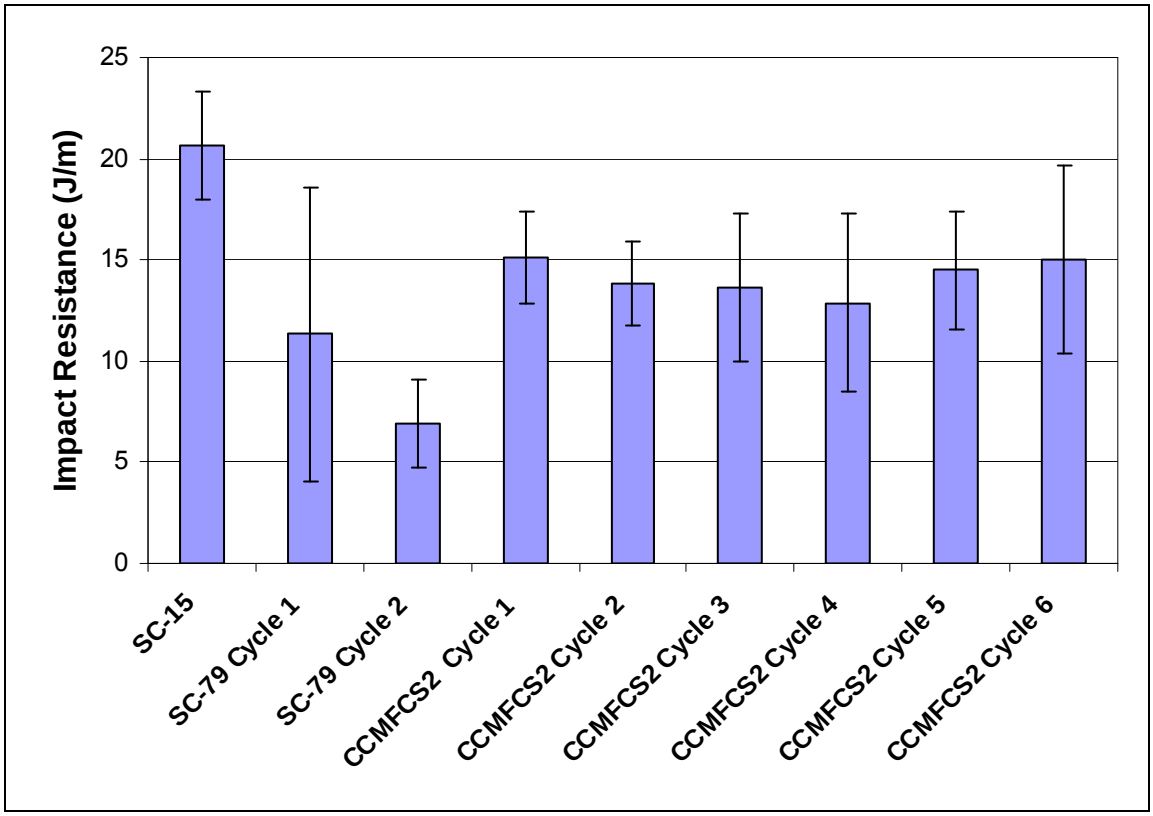

Figure 9. Impact resistance of notched samples.

For the unnotched samples, cycles 4–6 appear to have a slightly higher impact resistance than cycles 1– 3, similar to the results seen in the fracture toughness results (figure 10). Values for both SC-79 cycles follow the trend of the notched samples, with cycle 2 having the lowest overall value.

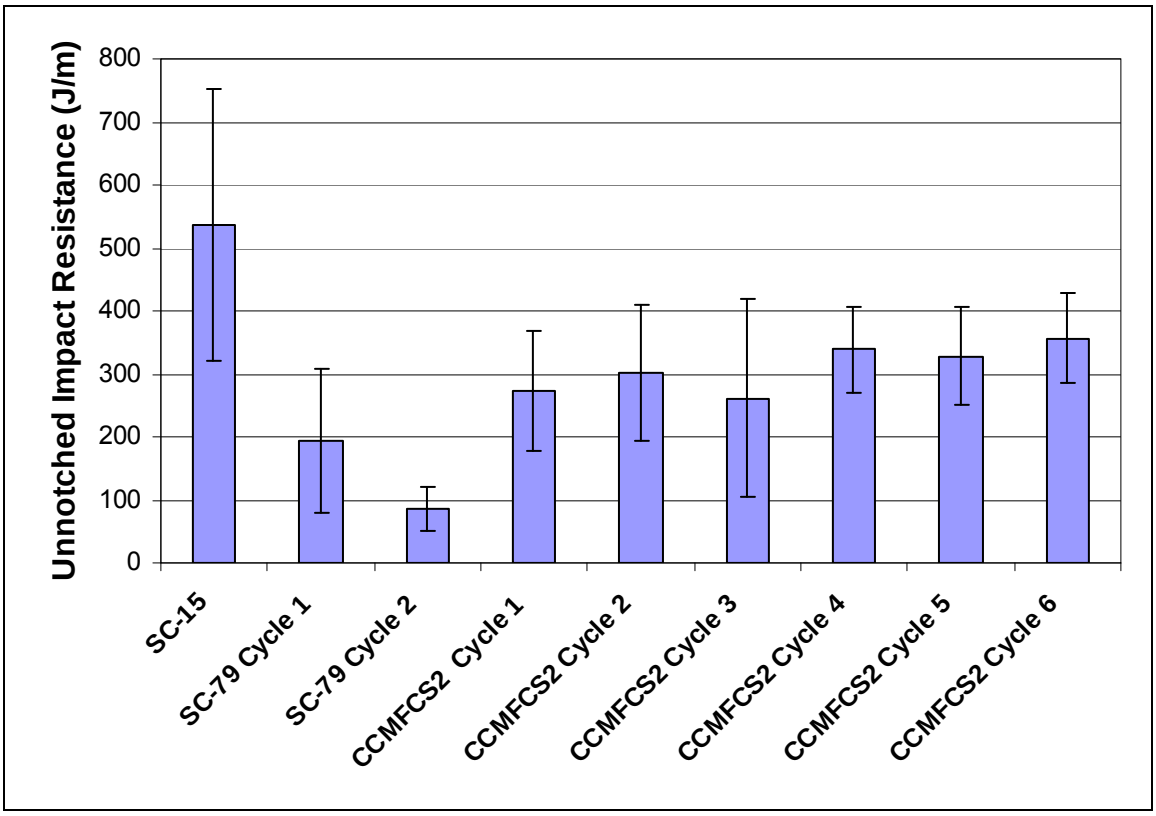

Figure 10. Impact resistance of unnotched samples.

In both notched and unnotched tests, SC-15 had the highest impact resistance while the SC-79 cycle 2 samples had the lowest. Again, SC-15's lower Tg helps the impact resistance and SC-79 cycle 2's high Tg hinders it. Unlike the fracture toughness results, SC-79 cycle 1 had the second lowest impact resistance. Other work has shown that increased fracture toughness correlates with increased impact toughness for toughened epoxies (*19*); however, if SC-79 cycle 2's fracture toughness was influenced more by the unreacted monomer than the toughening agent, that correlation may not apply. One large difference between the fracture and impact tests is the loading rate. In the Izod tests, the loading speed was several orders of magnitude higher than in the fracture testing, 1.4–2.3 m/s vs. 2×10^{-5} m/s. The impact test's loading rate is high enough to partially restrict the movement of the unreacted monomer, partially preventing its ability to absorb and dissipate the energy.

4. Discussion

Figure 11 clearly illustrates the relationship between Tg and fracture toughness. In general, as the Tg increases, the fracture toughness decreases. The CCMFCS2 cycles 4–6 show a more consistent trend than cycles 1–3. This is most likely due to the fact that 24 h at RT has the potential for more variation than 4 h in a temperature-controlled oven.

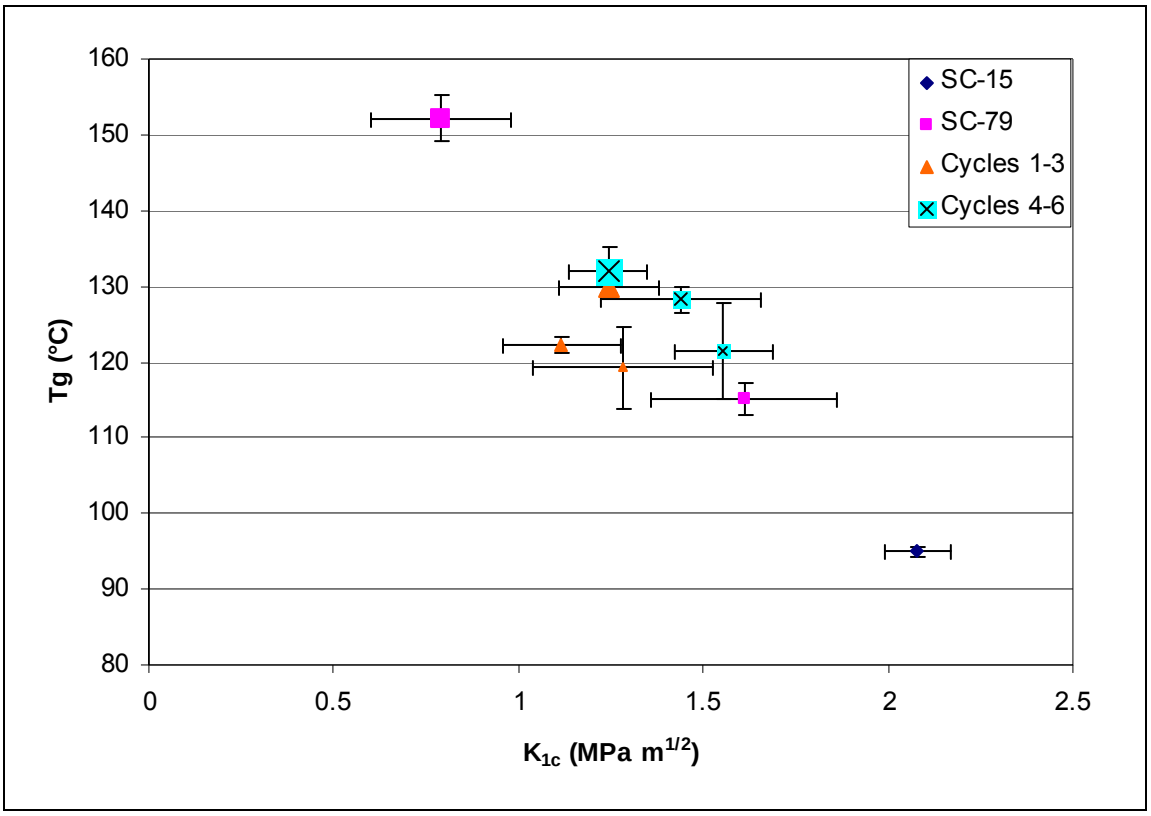

Figure 11. Tg vs. fracture toughness (K_{1c}); increasing symbol size corresponds to increasing cycle number.

Also, given that all CCMFCS2 cycles are clustered together, the different post-cures have only minor effects on the ultimate fracture toughness. A much larger difference is seen between the two cycles of SC-79, both in terms of Tg and fracture toughness.

The flexural strength and flexural moduli are compared in figure 12. A general trend of increasing strength with increasing modulus is seen; however, there is not a trend of increased post-cure temperature leading to increased strength and modulus. CCMFCS2 cycle 1 has the lowest strength and modulus.

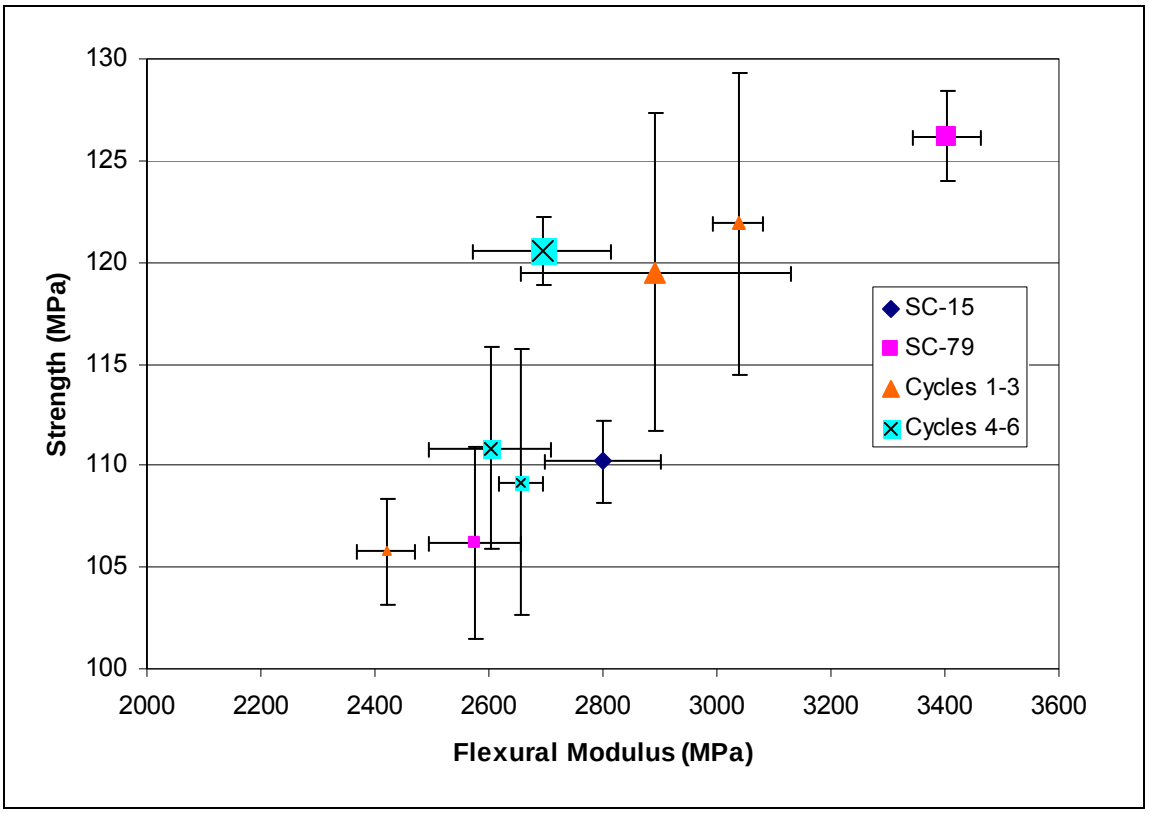

Figure 12. Strength vs. flexural modulus; increasing symbol size corresponds to increasing cycle number.

5. Summary and Conclusions

Two cure cycles of SC-79 and six cycles of CCMFCS were characterized and compared to SC-15. All resins have suitable viscosities for VARTM, though the slow viscosity rise during the 24-h cure time for CCMFCS2 cycles 1–3 is less desirable because of the increased potential for vacuum leaks, as well as the slower production rates.

Regardless of the cure cycle followed, the CCMFCS2 resin reached 96+% cure as measured by DSC. The lowest extents of cure occurred when the post-cure was only 121 °C. Extents of cure of 98.7+% were achieved whenever the post-cure temperature was 145 °C or higher. The SC-79 reached 91% and 95% cured for post-cures of 121 and 177 °C, respectively.

Large property differences exist between the two SC-79 cycles, while the differences between the six CCMFCS2 cycles are minor. The morphology changes very little between cycles, though the secondary phase appears slightly smaller for cycles 4–6 of CCMFCS2. The post-cure temperature has a greater influence on fracture toughness rather than the cure temperature. Higher fracture toughness can be achieved by sacrificing Tg by using a lower post-cure temperature.

SC-79 cycle 1 can provide a Tg above 110 °C with good fracture toughness, while cycle 2 provides a much higher Tg along with higher strength and modulus. The slow CCMFCS2 cycles 1–3 do not provide meaningful advantages over the much faster cycles 4–6. A decision between cycles 4–6 must be made given the desired properties. The highest Tg, modulus, and strength for CCMFCS2 can be achieved with a 177 °C post-cure, while the 145 °C post-cure gives only a slightly lower Tg, strength, and modulus but increased toughness. The maximum fracture toughness occurs with the 121 °C post-cure but also comes with lower modulus, strength, and Tg. Regardless of the resin or cycle chosen, the fracture toughness does not exceed that of SC-15, whereas all Tg's exceed that of SC-15.

6. References

1. McAninch, I. M.; Boyd, S. E.; La Scala, J. J. *Matrix Resin Screening for Composite Armor Applications*; ARL-TR-4825; U.S. Army Research Laboratory: Aberdeen Proving Ground, MD, May 2009.

2. Boyd, S. E.; McAninch, I. M.; Mulkern, T. *Evolution of Thermoset Matrix Composite Materials for Composite Armor Applications*; ARL-TR-4824; U.S. Army Research Laboratory: Aberdeen Proving Ground, MD, May 2009.

3. Applied Poleramic Inc. *SC-79: Toughened Dual Temperature Cure VARTM Resin* Technical Datasheet; Benicia, CA, July 2009.

4. Center for Composite Materials, University of Delaware. *CCMFCS2: 250–200 °F Curing Epoxy Matrix*; Newark, DE, April 2009.

5. Applied Poleramic Inc. *SC-15: Toughened Epoxy Resin System* Technical Datasheet; Benicia, CA, July 2009.

6. Lam, P. W. K. Characterization of Thermoset Cure Behavior by Differential Scanning Calorimetry. Part 1: Isothermal and Dynamic Study. *Polymer Composites* **December 1987**, *8* (6), 427–436.

7. ASTM Standard D 790-03. Standard Test Methods for Flexural Properties of Unreinforced and Reinforced Plastics and Electrical Insulating Materials. *Annu. Book ASTM Stand.* **2003**.

8. ASTM Standard D 5045-93. Standard Test Methods for Plane-Strain Fracture Toughness and Strain Energy Release Rate of Plastic Materials. *Annu. Book ASTM Stand.* **1993**.

9. ASTM Standard D 256-05. Standard Test Methods for Determining the Izod Pendulum Impact Resistance of Plastics. *Annu. Book ASTM Stand.* **2005**.

10. ASTM Standard D 4812-99. Standard Test Method for Unnotched Cantilever Beam Impact Resistance of Plastics . *Annu. Book ASTM Stand.* **1999**.

11. Pascault, J. P.; Sautereau, H.; Verdu, J.; Williams, R. J. J. *Thermosetting Polymers*. Marcel Dekker: New York, 2002.

12. Lin, K. F.; Yeh, R. J. Moisture Absorption Behavior of Rubber-Modified Epoxy Resins. *Journal of Applied Polymer Science* **2002**, *86*, 3718–3724.

13. Papanicolaou, G. C.; Kosmidou, T. V.; Vatalis, A. S.; Delides, C. G. Water Absorption Mechanism and Some Anomalous Effects on the Mechanical and Viscoelastic Behavior of an Epoxy System. *Journal of Applied Polymer Science* **2006**, *99*, 1328–1339.

14. Wisanrakkit, G.; Gillham, J. K. The Glass Transition Temperature (T_g) as an Index of Chemical Conversion for a High-T_g Amine/Epoxy System: Chemical and Diffusion-Controlled Reaction Kinetics. *Journal of Applied Polymer Science*, **1990**, *41*, 2885–2929.

15. Peterson, R. A.; Yee, A. F. Influence of Particle Size and Particle Size Distribution on Toughening Mechanisms in Rubber-Modified Epoxies. *Journal of Materials Science* **1991**, *26*, 3828–3844.

16. Yee, A. F.; Peterson, R. A. Toughening Mechanisms in Elastomer-Modified Epoxies: Part 1 Mechanical Studies. *Journal of Materials Science* **1986**, *21*, 2462–2474.

17. Selby, K.; Miller, L. E. Fracture Toughness and Mechanical Behavior of an Epoxy Resin. *Journal of Materials Science* **1975**, *10*, 12–24.

18. Peterson, R. A.; Yee, A. F. Toughening Mechanisms in Elastomer-Modified Epoxies: Part 3 The Effect of Cross-Link Density. *Journal of Materials Science* **1989**, *24*, 2571–2580.

19. Kong, J.; Ning, R.; Tang, Y. Study on Modification of Epoxy Resins With Acrylate Liquid Rubber Containing Pendant Epoxy Groups. *Journal of Materials Science* **2006**, *41*, 1639–1641.

NO. OF
COPIES ORGANIZATION

1 (PDF only) DEFENSE TECHNICAL INFORMATION CTR
DTIC OCA
8725 JOHN J KINGMAN RD
STE 0944
FORT BELVOIR VA 22060-6218

1 DIRECTOR
US ARMY RESEARCH LAB
IMNE ALC HRR
2800 POWDER MILL RD
ADELPHI MD 20783-1197

1 DIRECTOR
US ARMY RESEARCH LAB
RDRL CIM L
2800 POWDER MILL RD
ADELPHI MD 20783-1197

1 DIRECTOR
US ARMY RESEARCH LAB
RDRL CIM P
2800 POWDER MILL RD
ADELPHI MD 20783-1197

1 DIRECTOR
US ARMY RESEARCH LAB
RDRL D
2800 POWDER MILL RD
ADELPHI MD 20783-1197

ABERDEEN PROVING GROUND

1 DIR USARL
RDRL CIM G (BLDG 4600)

NO. OF
COPIES ORGANIZATION

1 LETTERKENNY ARMY DEPOT
M WANG
1 OVERCASH AVE
CHAMBERSBURG PA 17201

ABERDEEN PROVING GROUND

10 DIR USARL
RDRL WMM A
M MAHER
J WOLBERT
J CAIN
RDRL WMM B
S BOYD
RDRL WMM C
J LA SCALA
R JENSEN
I MCANINCH
RDRL WMP
S SCHOENFELD
RDRL WMP B
C HOPPEL
RDRL WMP E
S BARTUS